ISSN 2070-0504, Catalysis in Industry, 2013, Vol. 5, No. 4, pp. 283–296. © Pleiades Publishing, Ltd., 2013.

CATALYSIS IN CHEMICAL AND PETROCHEMICAL INDUSTRY

n-Decane Dehydrogenation on Bimetallic PtSn and PtGe Catalysts Prepared by Dip-Coating[1]

A. D. Ballarini, S. de Miguel, A. Castro, and O. Scelza

Instituto de Investigaciones en Catálisis y Petroquímica (INCAPE), Facultad de Ingeniería Química, Universidad Nacional del Litoral, CONICET, Santa Fe, Argentina

e-mail: aballa@fiq.unl.edu.ar

Received October 24, 2012

Abstract—The catalytic performance of Pt, PtSn and PtGe supported on γ-Al_2O_3 (γ-A) deposited by dip-coating of spheres of α-Al_2O_3 (α-A) is studied in the n-decane dehydrogenation. The effect of Sn and Ge addition to Pt on the activity and selectivity was analyzed. The catalytic characterization was carried out by using cyclohexane dehydrogenation (CHD), cyclopentane hydrogenolysis (CPH), temperature-programmed reduction (TPR), hydrogen chemisorption, X-ray photoelectron spectroscopy (XPS), thermogravimetric analysis (TGA) and scanning electronic microscopy (SEM). Pt(0.5)Sn/γ-A/α-A catalyst had the best catalytic performance and showed a low electronic interaction between the metals, with a surface segregation of Sn and the presence of oxidized Sn stabilized on the support. PtGe catalysts presented strong interactions with probable alloy formation. The catalytic performance of these catalysts is comparable to that reported in the patents.

Keywords: structured catalysts, dip-coating, n-decane dehydrogenation reaction, high paraffins

DOI: 10.1134/S2070050413040028

1. INTRODUCTION

The production of olefins is very important in the petrochemical and petroleum refining industries due to their application in several processes. One of the main sources of olefins is the thermal cracking of the petroleum crude (mainly for ethylene and propylene production) and, more recently, through catalytic processes. Taking into account the important demand of olefins, mainly those used for the production of polymers and fuel additives, and the high cost of thermal cracking equipment, there is an increasing interest in the development of new catalytic technologies to obtain high yield to olefins.

The tensioactive industry has become very important as well, since dodecylbenzene was found to have better properties than soaps. These detergents were initially produced by alkylation of benzene with tetramers of propene (mainly a mixture of C_{10}–C_{12} highly branched olefins) followed by sulfonation and neutralization with NaOH. This process decayed when evidence on the lack of biodegradability of these detergents was found [1–3]. From this finding, a new process appeared in the mid 60's, the production of sodium alkylbenzenesulfonate. This compound has an aliphatic linear chain of C_{10}–C_{14} [3, 4] which allows a fast biodegradation. These biodegradable detergents are synthesized by alkylation of benzene with linear α-mono-olefins of C_{10}–C_{14}. Taking into account the above mentioned characteristics, the production of these biodetergents at industrial scale was successful, thus displacing the preceding technologies. In this way the production of linear alkylbenzene or linear alkylbenzene sulfonate (LAB or LABS) increased significantly [3, 4].

This paper studies the production of 1-decene from the n-decane catalytic dehydrogenation using structured catalysts. For this purpose the catalyst must contain a dehydrogenating function, which is given by a noble metal (in our case Pt), though this component has hydrogenolytic properties, undesirable lateral process. In order to inhibit the hydrogenolytic capacity of the noble metals, an inactive second metal component, such as Sn or Ge, is added [5–11], to enhance the selectivity to olefins. γ-A/α-A (layers of γ-Al_2O_3 deposited on the periphery of the α-Al_2O_3 nucleus) was used as a support. It is known that γ-Al_2O_3 has acidic sites which catalyze the undesirable lateral reactions like cracking, isomerization and polymerization. The metallic function is responsible for the dehydrogenation capacity, while aromatization takes place through a bi-functional mechanism [8]. In this type of catalyst an acidic alumina has been used, but with the simultaneous addition of an alkaline metal (like Li) to poison the acidic sites so as to decrease the cracking capacity [8] and enhance the selectivity to olefins.

The increased importance of catalysts prepared by coating [12] is due to the advantages derived from the

[1] The article is published in the original.

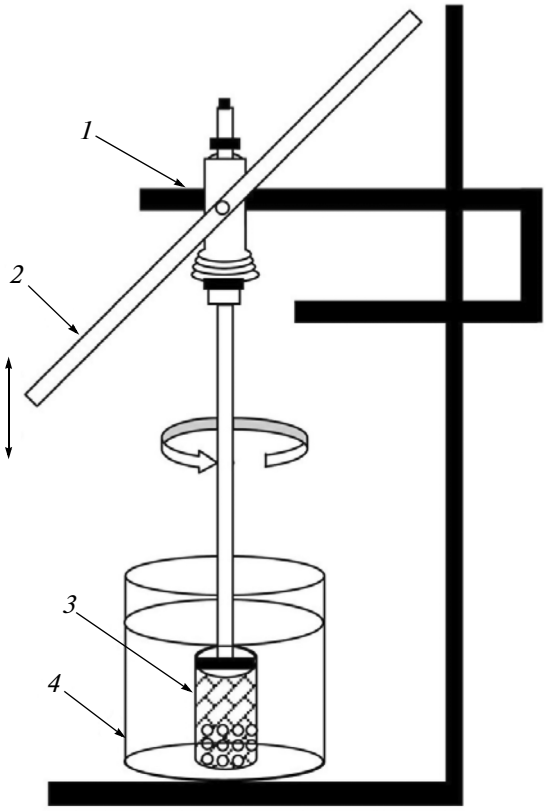

Fig. 1. Diagram of equipment for the deposition of "Coating": *1*—mechanical stirrer, *2*—level to up and down the basket, *3*—rotating metallic basket, *4*—gel containment vessel.

good mass and heat transfer [13] which increase the energetic efficiency and the heat recovery [14]. According to the literature, there are different procedures for coating which include washcoating [15–18], dip-coating [17–31], spraying [16], plasma spraying [19, 26], granulation [27], deposition without electrodes [30], coating based on polymers [31], chemical vapor deposited layer (CVD) and physical vapor deposited (PVD) layers [17]. In all cases the objective of this work is related with the production of a uniform thin layer, with both high thermal resistance and specific surface area, free of crack and capable of maintaining the integrity and durability of the system substrate/coating under the operation conditions.

The catalysts preparation is carried out by an efficient and simple method to achieve the washcoating on a very complex and spherical geometry. The methodology involves the use of fewer number of elements, what represents an economical advantage, with respect to the catalytic formulations reported in patents [32–35]. The supports consisted of a thin layer of γ-Al_2O_3 (10–20 μm of thickness) deposited on nonporous α-Al_2O_3 spheres (support named γ-A/α-A). This support was prepared by the dip-coating method using boehmite gel for the coating. Besides, the incidence of the dip-coating preparation method on the activity, selectivity and yield of bimetallic PtSn and PtGe supported on γ-A/α-A in the selective n-decane dehydrogenation to 1-decene were studied.

Furthermore, the effect of the second metal loading added to Pt (Sn – 0.3 or 0.5 wt %, and Ge – 0.18 or 0.3 wt %) on the catalytic properties was analyzed. The effect of the Li addition to γ-A/α-A was also explored. Finally, a correlation between the physicochemical properties and the catalytic behavior in n-decane selective dehydrogenation was obtained by means of different characterization techniques, such as XRD, TPR, hydrogen chemisorption, test reactions of the metallic phase, XPS and TPO for carbon determination.

2. EXPERIMENTAL

2.1. Preparation of the Supports: γ-A/α-A and γ-A/α-A-Li

A layer of γ-Al_2O_3 was deposited on α-Al_2O_3 CERALOX (substrate) with the following characteristics: bulk density – 0.83 g mL^{-1}, mean sphere diameter – 0.95 cm, specific surface area (S_{BET}) – 4.70 $m^2 g^{-1}$, mean pore size – 1.44 nm. The deposition of a thin layer of γ-Al_2O_3 on the substrate included the following steps:

2.1.1. Pretreatment of the support. A thermal treatment at 500°C in air for 3 h to stabilize the phase. This thermal treatment was followed by a chemical one using HCl_{aq} (1 N for 24 h) in order to develop surface rugosity, which favoured the adherence and stability of the γ-Al_2O_3 layers. The ratio between the volume of aqueous HCl solution and the mass of α-Al_2O_3 was 1.4 mL g^{-1}. After this treatment the substrate was washed with distilled water in order to eliminate chlorine. Then the sample was submitted to a drying step at 120°C for 12 h and finally calcined at 500°C for 3 h;

2.1.2. Preparation of the boehmite gel. The gel consisted of aggregates of the charged colloid particles producing a uniform network [24]. The boehmite gel (in nitric acid media) was prepared using the commercial boehmite Disperal P2, the concentration of boehmite being 10 wt % and that of HNO_3 equal to 0.2 N;

2.1.3. Deposition of boehmite on the substrate. For this purpose, the dip-coating method was used. The spheres of α-Al_2O_3 were introduced in a rotating (80 r min^{-1}) cylindrical vessel. The cylindrical wall and the base of this vessel were made with a mesh of steel (Fig. 1). The vessel with the spheres was introduced into the boehmite gel maintaining the rotation for 1h. This procedure was repeated two times in order to increase the thickness of the deposited layers. After the deposition of the layers of boehmite, the vessel was retired from the gel with a rate of 0.015–0.02 cm min^{-1}. Then the vessel was suspended until finishing the drip of the gel. The spheres were dried with air flow in two steps: one at slow drying rate (5 m s^{-1} of air flow) for 0.5 h at high temperature (50°C) and the other with a

fast drying rate (10 m s^{-1} of air flow) for 0.5 h at low temperature (30°C);

2.1.4. Thermal treatments of the samples. This treatment is carried out in order to transform the deposited boehmite into γ-Al_2O_3 [36]. The substrate covered by a layer of boehmite was dried at 120°C for 12 h and then calcined at 500°C. The resulting specific surface area of the γ-Al_2O_3 layer was 282 $m^2 g^{-1}$ and the thickness of layers was about 10–20 μm.

The γ-A/α-A-Li (0.1 wt %) support was prepared by doping γ-A/α-A with an aqueous solution of LiOH (Aldrich, 99%) so as to obtain a final Li loading of 0.1 wt %. The ratio of Li solution volume to mass of support was 1.4 mL g^{-1}. After impregnation the sample was dried at 120°C and finally calcined at 500°C for 3 h.

2.2. Preparation of Pt(0.3 wt %)/γ-A/α-A

The monometallic Pt catalyst was prepared by immersion of the spheres of the substrate with the layers of γ-Al_2O_3 deposited on the periphery of α-Al_2O_3 into an aqueous solution of H_2PtCl_6. The concentration of the H_2PtCl_6 (Aldrich, 99%) solution was such as to obtain the desired Pt loading (0.3 wt %). The impregnation volume/weight of the support ratio was 1.4 mL g^{-1}. The impregnation was carried out at room temperature for 6 h. Then the solid was dried at 120°C for 12 h and finally calcined at 500°C for 3 h. The monometallic catalyst was called ***Pt/γ-A/α-A***.

2.3. Preparation of PtSn(0.3 or 0.5 wt %)/γ-A/α-A and PtGe(0.18 or 0.3 wt %)/γ-A/α-A Catalysts

Bimetallic Pt(0.3 wt %)Sn(0.3 or 0.5 wt %) catalysts were prepared by successive impregnation of the corresponding support (γ-A/α-A) with an aqueous solution of H_2PtCl_6, dried at 120°C for 12 h and then impregnated with hydrochloric solution (1.2 M) of $SnCl_2$. Bimetallic Pt(0.3 wt %)Ge(0.18 or 0.3 wt %) catalysts were also prepared by successive impregnation of the corresponding support with an aqueous solution of H_2PtCl_6, dried at 120°C for 12 h and then impregnated with a hydrochloric solution of $GeCl_4$. In both cases, the impregnations were carried out at room temperature for 6 h, the impregnating volume/support weight ratio being 1.4 mL g^{-1} and the concentrations of the impregnating solutions of the Pt, Sn and Ge precursors were such as to obtain the desired Pt, Sn and Ge contents. After impregnation, samples were dried at 120°C for 12 h, and calcined in air at 500°C for 3 h. It must be noted that the Sn contents were equimolar with those corresponding to the Ge contents. The bimetallic catalysts were called ***PtSn(0.3* or *0.5)/γ-A/α-A*** and ***PtGe(0.18 or 0.3)/γ-A/α-A***.

2.4. Support Characterization

The support characterizations were carried out by determining the textural characteristics of the substrates and the deposited layers. X-ray diffraction, SEM measurements and TPD of pyridine were also used.

The specific surface area (S_{BET}) and the mean ratio pore size of both the substrate and the deposited layer were obtained using an Accusorb 2100E Micromeritics equipment. The samples were first outgassed at 200°C for 2 h at 10^{-4} mm Hg. The dead volume of the equipment was determined with helium (AGA, 99.999%) at the temperature of liquid nitrogen. The isotherms were measured at 77 K using nitrogen as adsorbate in the range of pressure between 35 and 150 mm Hg, and the S_{BET} was obtained by linearizing the BET equation.

The samples (powders) were analyzed in a Shimadzu X-ray diffractometer using a Cu K_α radiation, voltage 30 kV, current of 30 mA, opening of divergence and dispersion of 2°, and a continuous scanning. The XRD pattern was taken between 10 and 80°. The diffraction lines were compared with the standard JCPDS in order to identify the detected species.

The uniformity of the layers deposited by coating was determined by scanning electronic microscope (SEM) using a JSM-35C JEOL equipment, connected to a SemAfore acquisition system of digital images operated at 2 kV. Samples were covered with a gold film (deposited by sputtering with a evaporator VEECO, model VE-300, operated in argon atmosphere) before the analysis. The measurements were carried out under the mode of secondary electrons image, using 20 kV as an acceleration voltage.

For the TPD of pyridine experiments, the sample (0.200 g) was previously impregnated with an excess of pyridine (Merck, 99.9%) for 4 h. The excess of pyridine was eliminated under vacuum at room temperature to obtain a dried powder. Then the samples were put into a quartz reactor and a nitrogen flow of 40 mL min^{-1} was passed through the bed. The pyridine weakly adsorbed was eliminated at 110°C for 2 h. Then the sample was heated from 110°C up to 500°C at a heating rate of 10°C min^{-1}. The amount of desorbed pyridine during the TPD experiments was measured by connecting a FID detector in the exhaust of the reactor. In the same way, the TPD of pyridine was measured on the commercial γ-Al_2O_3 CK 300.

2.5. Characterization of the Metallic Phase

The characteristics of the metallic catalysts were determined by test reactions: cyclohexane (CH) dehydrogenation (CHD) and cyclopentane (CP) hydrogenolysis (CPH); hydrogen chemisorption, temperature-programmed reduction (TPR) and X-ray photoelectron spectroscopy (XPS).

The tests reactions of the metallic phase were carried out in a differential flow reactor with H_2/CH and

H_2/CP molar ratios of 26 and 22, respectively. The temperature was 400°C for the first reaction and 500°C for the second one. The reaction products were analyzed by gas chromatography with a Chromosorb column and a FID detector. The catalysts were previously reduced at 500°C under flowing hydrogen (60 mL min^{-1}). The activation energies were obtained from slope of the curve ln R^0 vs $1/T$ (T – temperature, K). R^0 was calculated from the conversion obtained at three different temperatures. The sample mass was chosen to obtain a conversion less than 5%, condition in which the reactor can be considered as a differential one.

Hydrogen chemisorption measurements were made in a volumetric equipment. The sample weight used in the experiments was 0.300 g. The sample was outgassed at room temperature, heated under flowing H_2 (60 mL min^{-1}) from room temperature up to 500°C, and then kept at this temperature for 2 h. Then, the sample was outgassed under vacuum (10^{-4} mm Hg) for 2 h. After the sample was cooled down to room temperature (25°C), the hydrogen dosage was performed in the range of 25–100 mm Hg. The isotherms were linear in the range of used pressures. The amount of chemisorbed hydrogen was calculated by extrapolation of the isotherm to pressure zero.

Temperature-programmed reduction (TPR) experiments were carried out in a quartz flow reactor. The samples (0.500 g) were heated at 6°C min^{-1} from room temperature up to 800°C. The reductive mixture, H_2 (5%v/v)-N_2 was fed to the reactor with the flow rate of 10 mL min^{-1}. Catalysts were previously calcined *in situ* at 500°C for 3 h with an air flow rate of 160 mL min^{-1}.

XPS measurements were carried out in a SPECS spectrometer, which operates with an energy power of 50 eV (radiation Mg K_α, $h\nu$ = 1253.6 eV for PtSn or radiation Al K_α, $h\nu$ = 1486.6 eV for PtGe). The pressure of the analysis chamber was kept at 4×10^{-10} mm Hg. Samples were previously reduced in hydrogen at 500°C for 3 h. Binding energies (BE) were referred to the C1s peak at 284.9 eV. The peak areas were estimated by fitting the experimental results with Lorentzian–Gaussian curves by using CASA XPS software.

To quantify the carbonaceous deposits, the profiles of temperature-programmed oxidation (TPO) on catalysts before and after the n-decane dehydrogenation reaction were determined using the thermogravimetric analysis (TGA) technique. The experiments were carried out on the SDTA Mettler STAR^e. Fresh (used as a reference) and used catalysts were stabilized under nitrogen flow at 250°C for 1 h before starting the experiments of TPO. The samples (0.010 g) were heated at 5°C min^{-1} from 250 to 500°C under air flow.

2.6. Catalytic Test in n-Decane Dehydrogenation

The catalysts (0.500 g) were tested in the n-decane dehydrogenation reaction in a continuous flow reactor at 465°C and 0.1 MPa. The reactor was fed with a mixture of H_2 and $C_{10}H_{22}$ (molar ratio $H_2/C_{10}H_{22}$ = 4) using a LSVH = 40 h^{-1}. Prior to the reaction, samples were reduced with hydrogen at 500°C for 3 h. The reaction products were analyzed along the reaction time using a GC chromatograph with a FID detector coupled to a PONA column. The reaction products detected by chromatographic analysis were:

(1) gaseous products (<C_5);

(2) light paraffins (C_5–C_9) produced by cracking reactions;

(3) 1-decene or α-C_{10} monolefins;

(4) other mono-olefins (positional isomers, conjugated and non-conjued diolefins, n-dienes, n-trienes, excluding 1-decene;

(5) non-linear hydrocarbons (this group includes: iso-paraffins, iso-olefins, cyclization products, aromatics, alkyl aromatics, etc.). In all cases the liquid yield (<C_5) ranged between 98 and 99%.

The n-decane conversion was calculated as the sum of the chromatographic areas of all products (except H_2) affected by the corresponding response factors. The selectivity to different groups of products (S_j) was defined as follows:

$$S_j = n_j \Big/ \sum n_j,$$

where n_j is the number of moles of product j; $\sum n_j$ is the total number of moles of the products (except H_2).

The yield to 1-decene ($Y_{1\text{-}decene}$) was defined as:

$$Y_{1\text{-}decene} = AS_{1\text{-}decene},$$

where A is the total conversion; $S_{1\text{-}decene}$ is the selectivity to 1-decene.

Conversions, selectivities and yields were calculated at different reaction times (10–120 min). It is worth noticing that even though the catalysts were tested at conversions between 2 and 13%, no important selectivity changes were obtained at different conversions.

3. RESULTS AND DISCUSSION

3.1. Support Characterization

Figure 2 shows the microphotography of the transversal section of α-Al_2O_3 covered by layers of γ-Al_2O_3 (γ-A/α-A). The thickness of the γ-Al_2O_3 deposited layers was about 10–20 μm. Besides, the S_{BET} of the substrate and the deposited layer by coating were determined, being 4.70 and 282 $m^2 g^{-1}$, respectively. In order to verify the deposition of layers of gamma alumina, a XRD determination after the thermal treatment at 500°C was made and the spectrum is shown in Fig. 3. It can be only observed the characteristic lines of γ-Al_2O_3 (File № 10-0425). The presence of other transition alumina could be possible. To verify the layer stability, the adherence of the alumina layer on the supports has been evaluated too. The ultra-sonic test in hydrocarbon media [37] has resulted in a loss of

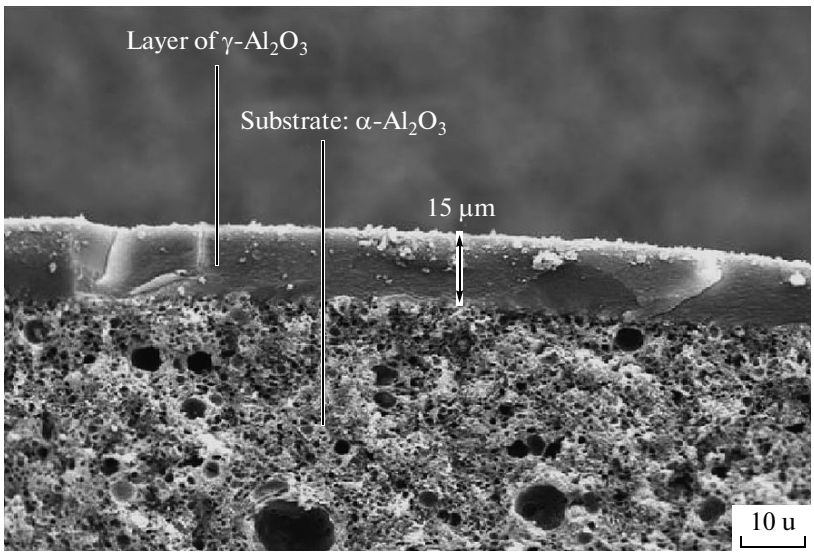

Fig. 2. Transversal section of a α-Al_2O_3 sphere with the γ-Al_2O_3 layers deposited by dip-coating. Sample γ-A/α-A.

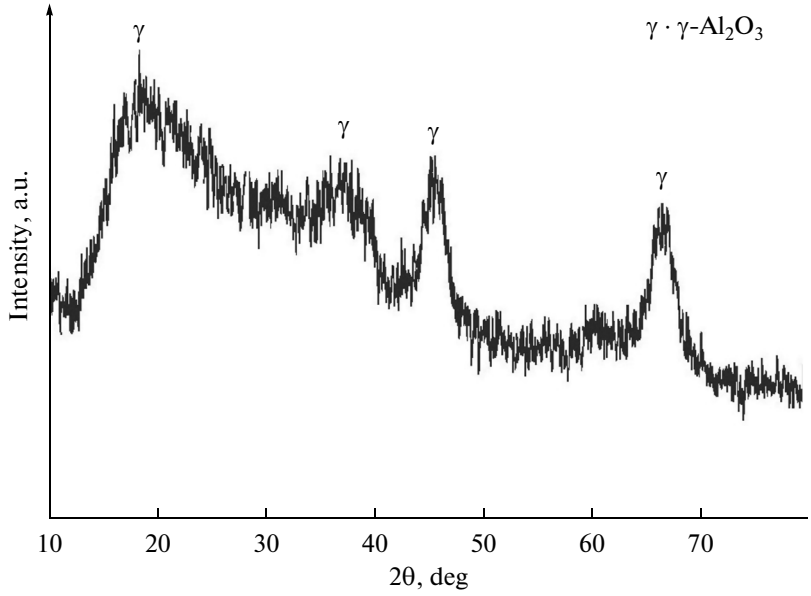

Fig. 3. XRD spectrum of the deposited γ-Al_2O_3 layers.

weight of about 0.5–0.7% of the original weight of the deposited layers.

The Li-doped support (γ-A/α-A-Li) was obtained by impregnation of γ-A/α-A with a salt of the alkali metal. On the doped and undoped supports the acidic properties were determined by TPD of pyridine (TPDP). Figure 4 shows the TPDPs for γ-Al_2O_3 CK 300, γ-A/α-A and γ-A/α-A-Li. The low acidity of γ-A/α-A could be due to the fact that γ-A (deposited on α-A) is produced by the thermal decomposition of boehmite [AlO(OH)] at 500°C, and it is probable that under these treatment conditions a complete dehydroxilation is not reached, thus producing a γ-Al_2O_3 with low acidity. This effect can explain the low difference in the acidity between γ-A/α-A and γ-A/α-A-Li. Taking into account these results, the Li addition to γ-A/α-A can be avoided since it does not modify the acidity of the support in a way that it could decrease the undesirable lateral reaction of coking and polymerization in an important magnitude.

3.2. PtSn Catalysts Characterization

The study of the metallic phase of Pt and PtSn catalysts supported on γ-A/α-A was first carried out by TPR. Fig. 5, a shows the TPR profiles of PtSn(0.3 and

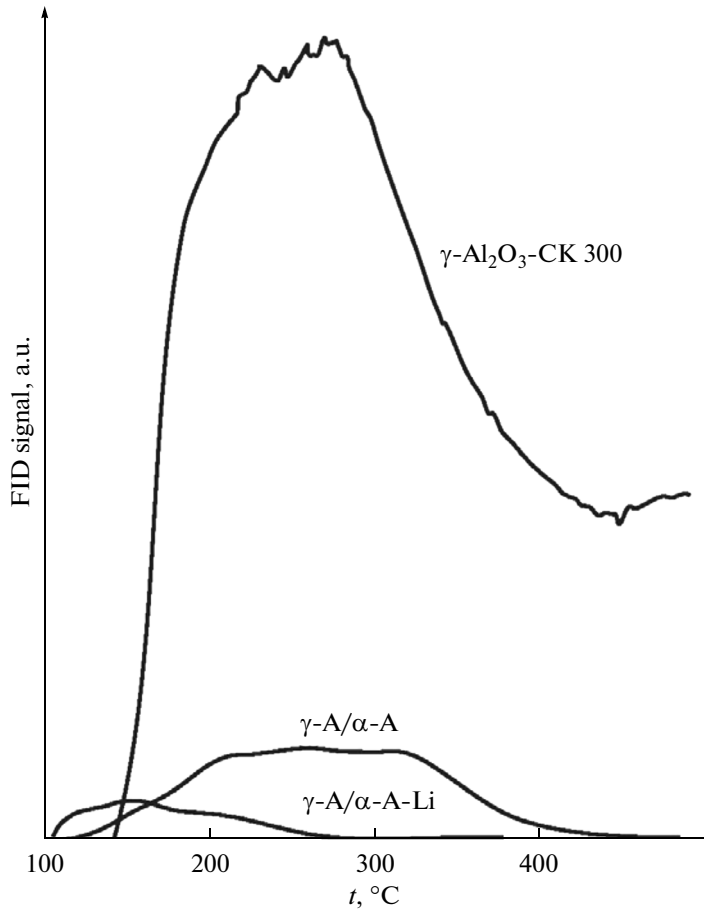

Fig. 4. TPD of pyridine for different samples (layers of γ-A, γ-A-Li and γ-Al_2O_3 CK 300).

0.5 wt %) catalysts previously calcined at 500°C as well as those of the supported monometallic catalysts (Pt and Sn). The Pt/γ-A/α-A catalyst shows two reduction peaks, one at 250°C which can be assigned to Pt oxide reduction, and another one with a lower intensity placed at 400°C, that could be attributed to different Pt-oxychlorinated species [38]. The Sn(0.5 wt %)/γ-A/α-A catalyst displays a broad peak placed at temperatures higher than 450–500°C. In the study of PtSn/γ-A/α-A catalysts, it is observed that when Sn is added to Pt/γ-A/α-A catalyst the main reduction peak is shifted to higher temperatures (250–280°C) and the peaks are broader when the Sn loadings are higher. The broadening of the first peak could be due to a co-reduction of both metals or alloy formation. Moreover, a second broad reduction peak at $T >$ 450°C can be observed in PtSn catalysts, which can mainly be attributed to the reduction of Sn oxidized species stabilized on the support.

Besides, the test reactions of the metallic phase, cyclohexane dehydrogenation (CHD, structure-insensitive reaction [39, 40]) and cyclopentane hydrogenolysis (CPH, structure-sensitive reaction [41–44]) were performed in order to study the state of the metallic phase. It should be noted that Sn is inactive for the above mentioned reactions. Table 1 shows the values of the initial reaction rate of CHD (R^0_{CH}) and CPH (R^0_{CP}), the activation energy in CHD and the chemisorbed hydrogen (V_{H_2}) for the different catalysts. It can be observed that the addition of increasing amounts of Sn to Pt/γ-A/α-A catalyst produces the consequent decrease of the dehydrogenating activity, according to the decrease of R^0_{CH}. It must also be indicated that the Sn addition to Pt does not lead to a significant modification of the activation energy of CHD. This behavior would indicate that there is no important electronic modification of Pt by Sn. It is also observed that the Sn addition to Pt markedly decreases the hydrogenolytic capacity of the metallic phase. Taking into account that this is a structure-sensitive reaction, which needs the ensemble of several Pt atoms, it can be concluded that the decrease of the CPH rate by the Sn addition to Pt is due to a geometric effect of Sn species on Pt ones (dilution or blocking). The decrease of the chemisorbed hydrogen by the Sn addition to the monometallic catalyst would also indicate a geometric effect.

In order to study in more detail the state of the metallic phase, XPS measurements were carried out

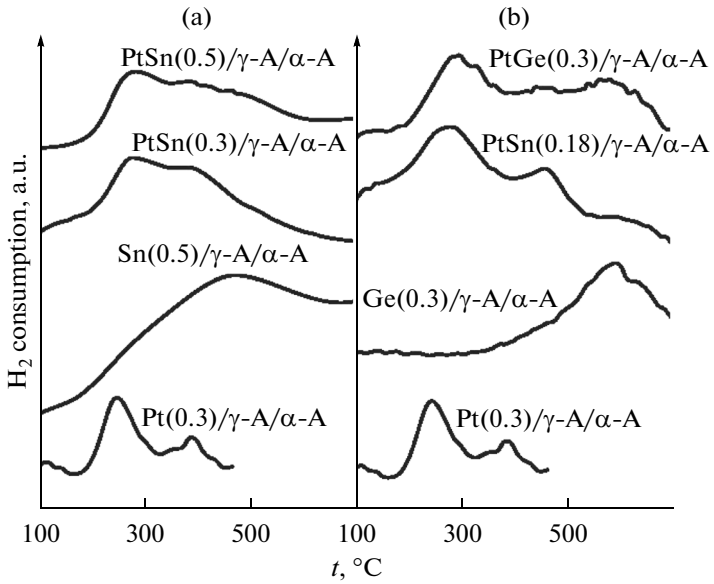

Fig. 5. TPR profiles of PtSn(0.3 and 0.5 wt %) (a) and PtGe(0.18 and 0.3 wt %) catalysts supported on γ-A/α-A (b). TPR of monometallic ones are added as reference.

on samples previously reduced in hydrogen at 530°C. The experiments were performed on PtSn(0.5 wt %)/γ-A/α-A (level Sn3*d*). In the XPS spectra of the Pt 4d level for PtSn/γ-A/α-A, a doublet can be observed at 313.5 and 314 eV corresponding to zerovalent Pt [44]. The XPS spectrum of Sn3*d* presents two peaks, as shown in Fig. 6. The first peak at 483.0 eV can be attributed to Sn(0) while the second peak at 485.8 eV can be assigned to Sn(II–IV) species. It must be noted that the difference of binding energies (*BE*) between Sn(II) and Sn(IV) is very small [44]. Hence, it is not possible to discriminate these species from XPS results. Table 2 shows that the percentage of Sn(0) calculated form XPS experiments was 4 % for this catalyst and the Sn/Pt surface atomic ratio was 5.4, which indicates a surface Sn enrichment of the metallic phase since the atomic Sn/Pt_{bulk} ratio was 2.7.

XPS results confirm that the metallic phase of these PtSn/γ-A/α-A catalysts appears to be composed by free Pt(0) particles, Pt particles blocked and/or diluted by Sn, a small concentration of alloyed particles and oxidized Sn particles stabilized on the support. These results are in agreement with the ones obtained from reaction tests, hydrogen chemisorption and TPR. Moreover, it must be indicated that for these bimetallic catalysts, a fraction of Sn would be segregated on the surface of the metallic phase in a way similar to those supported on γ-Al_2O_3 [46, 47].

3.3. PtGe Catalysts Characterization

Figure 5b shows the TPR profiles of PtGe(0.18 and 0.3 wt %) catalysts supported on γ-A/α-A previously calcined at 500°C. The TPR profiles of Pt and Ge supported monometallic catalysts are also shown as reference. In the Ge(0.3 wt %)/γ-A/α-A catalyst, a broad reduction peak with a maximum at about 600–650°C was found which can be attributed to the reduction of Ge^{+4} species [48]. In the case of bimetallic PtGe/γ-A/α-A catalysts, the first reduction

Table 1. Initial reaction rates in CHD and CPH, activation energy of CHD and chemisorbed hydrogen for Pt, PtSn and PtGe catalysts supported on γ-A/α-A

Catalyst	Initial reaction rates, mol/(h g catal.)		Activation energy in CHD, kJ/mol	Chemisorbed hydrogen (V_{H_2}), mL H_2 STP/g catal.
	R^0_{CH} (400°C)	R^0_{CP} (500°C)		
Pt	67.6	3.00	25	4.6
PtSn(0.3)	33.0	0.70	19	2.0
PtSn(0.5)	9.9	0.05	21	2.2
PtGe(0.18)	30.4	0.07	54	1.4
PtGe(0.3)	15.9	0.05	50	1.7

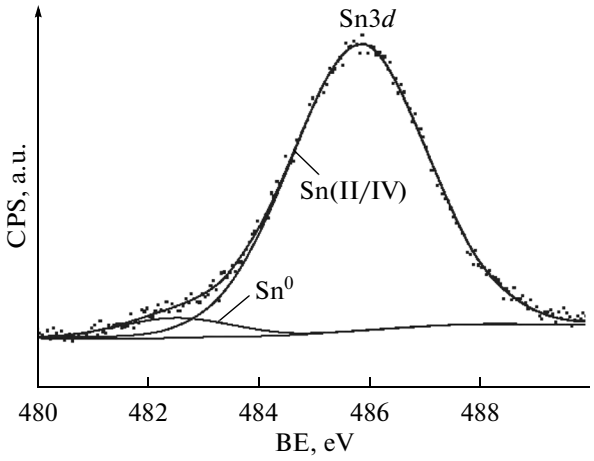

Fig. 6. XPS signals of Sn3*d* in the PtSn(0.5)/γ-A/α-A catalyst.

peak is slightly shifted at higher temperatures with respect to that of the monometallic one. Besides, this peak broadens when the Ge loading increases. This first reduction peak can be attributed to a Pt and Ge co-reduction with probable alloy formation. In the PtGe/γ-A/α-A catalyst, a reduction zone can be observed at temperatures where Ge is reduced in the monometallic Ge catalyst. This zone can be assigned to the reduction of Ge species stabilized on the support.

Table 1 shows the values of the initial reaction rate of CHD (R^0_{CH}) and CPH (R^0_{CP}), the activation energy in CHD and the chemisorbed hydrogen (V_{H_2}) for the different catalysts. It should be noted that Ge is also inactive for the above mentioned reactions. When increasing amounts of Ge are added to Pt/γ-A/α-A catalyst, an important decrease of the CHD rate is observed with respect to the monometallic ones. An important increase of the activation energy in CHD also takes place, which would indicate an important interaction between Pt and Ge with probable alloy formation with charge transfer from Pt to the promoter. The important decrease of the CPH rate when Ge is added to Pt can be interpreted as the strong decrease of the concentration of Pt ensembles by alloy formation and also by a probable blocking/dilution effect of Ge on Pt sites. In this case, taking into account the increase of the activation energy in the CHD, an alloy formation between Pt and Ge could be considered, in contrast with the results observed for the PtSn/γ-A/α-A system. It must be noted that the strong decrease of the CPH rate is simultaneously followed by a strong decrease of the chemisorbed hydrogen. The hydrogenolytic capacity strongly decreases when Sn or Ge loadings increase, these effects being more pronounced for Ge addition. Castro et al. [6] found that the addition of Sn, Ge and Pb to the Pt/γ-Al_2O_3 catalyst leads to an important decrease of the hydrogenolytic capacity of the metallic phase.

Table 2. Binding energies, bulk and XPS surface atomic Sn/Pt and Ge/Pt ratios for the different samples supported on γ-A/α-A

Catalyst	Binding energies (*BE*), eV		Atomic ratios (Sn/Pt or Ge/Pt)	
	Sn3$d_{5/2}$	Ge3$d_{5/2}$	bulk	surface
PtSn(0.5)	483.0 Sn° (4%) 485.8 Sn(II/IV) (96%)	–	2.8	5.4
PtGe(0.3)	–	28.5 Ge° (58%) 30.4 Ge(II/IV) (42%)	2.8	4.2

In this way, for PtGe/γ-A/α-A catalyst it is possible to postulate that the metallic surface is composed by alloy particles with low dehydrogenation and hydrogenolytic capacities [48–53], particles of oxidized Ge blocking or diluting the Pt clusters, Ge oxidized species stabilized on the support and probably particles of free Pt(0). The literature [49, 50] indicates that Ge is reduced to Ge(0) in PtGe/Al_2O_3 catalyst and this Ge(0) species would have a strong interaction with Pt and could form alloys or PtGe clusters. In these alloyed particles Ge could increase the electrophilic character of Pt.

Besides, XPS measurements on PtGe(0.3 wt %)/γ-A/α-A (level Ge3*d*5/2) were carried out on samples previously reduced at 530°C in hydrogen. The XPS spectra of the Pt4*d* level for this bimetallic catalyst also display the doublet at 313.5 and 314 eV, which corresponds univocally to Pt(0) [44]. The XPS experiments of the Ge3$d_{5/2}$ level showed two peaks at 28.5 and 30.4 eV, respectively, as shown in Fig. 7. The first peak can be assigned to Ge(0) species and the second one to Ge(II–IV). It is to be noted that Ge(II) and Ge(IV) signals cannot be discriminated since the BE of both Ge oxides are very close [44]. From XPS results it was possible to determine the percentage of the reduced and the oxidized species, resulting 58.5% for Ge(0) and the remaining value corresponds to Ge(II–IV). Moreover, from Table 2 it can be observed that there is a surface Ge enrichment (surface atomic ratio Ge/Pt = 4.21 and bulk atomic ratio Ge/Pt = 2.8). The results also show the existence of an important amount of Ge(0), which can be alloyed with Pt, together with an important fraction of oxidized Ge, which can be placed both in the metallic phase and on the support. These conclusions confirm the results obtained from test reactions, hydrogen chemisorption and TPR. It should be remarked that PtGe catalysts would show an impor-

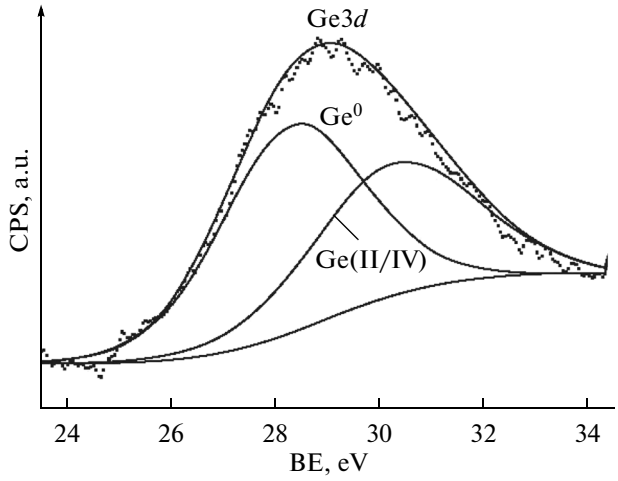

Fig. 7. XPS signals Ge3*d* in the PtGe(0.3)/γ-A/α-A catalyst.

tant fraction of intermetallic alloys, much higher than PtSn.

These latter results are in agreement with those reported in the literature for other supports. Thus, Borgna et al. [51] found that the Ge addition to Pt in catalysts supported on γ-Al_2O_3 produces an increment of the electrophilic character of Pt and it also geometrically modifies the surface Pt with the consequent decrease of the dehydrogenation activity. De Miguel et al. [50] reported that in PtGe/γ-Al_2O_3 catalysts, small amounts of free Pt would exist and the alloyed phase would be important. Moreover, a certain blocking effect of Pt by Ge was also found.

3.4. Catalytic Test in n-Decane Dehydrogenation

Monometallic and bimetallic catalysts (PtSn and PtGe with different Sn or Ge contents) supported on γ-A/α-A were tested in n-decane dehydrogenation at 465°C using a continuous flow equipment. Figure 8 shows the initial (X^0) conversion of n-decane (at 10 min of the reaction time) and final conversion (X^f) measured at 120 min of reaction time. It can be observed that all the bimetallic catalysts display a better activity than the monometallic one except the PtGe(0.18)/γ-A/α-A catalyst which displays a behavior very similar to the monometallic catalyst.

It can also be observed that the PtSn catalysts show a better conversion than the PtGe series. For both catalyst series the n-decane total conversion (initial and final ones) is higher when the Sn or Ge loadings increase. Moreover, the apparent increase of the initial activity (n-decane conversions) of bimetallic catalysts with respect to the monometallic one can be related to the electronic and/or geometric modification of Pt by Sn or Ge addition. It is expected that in the first steps of the reaction the monometallic catalyst can be more active than the bimetallic ones, but in the first reaction steps the carbon deposition on the monometallic catalyst can be higher than in the bimetallic ones producing a higher catalyst deactivation of Pt (in Pt/γ-A/α-A catalyst) with the consequent activity loss. This behavior was found in propane and n-butane dehydrogenation using pulse techniques on PtGe and PtSn catalysts supported on doped alumina, spinels of Mg or Zn and catalysts prepared by dip coating [23, 54–62]. According to the results obtained by the characterization of the metallic phase of the bimetallic catalysts, PtGe catalysts would show an important fraction of intermetallic alloys (much higher than PtSn) but a poorer catalytic performance, which could be due to the different alloy concentrations in both catalysts. It must be noted that dehydrogenation reaction is carried out on the surface of platinum and the side reactions of cracking and isomerization are mainly performed by a bifunctional mechanism that involves the acid centers of the catalysts, i.e. on the support and the

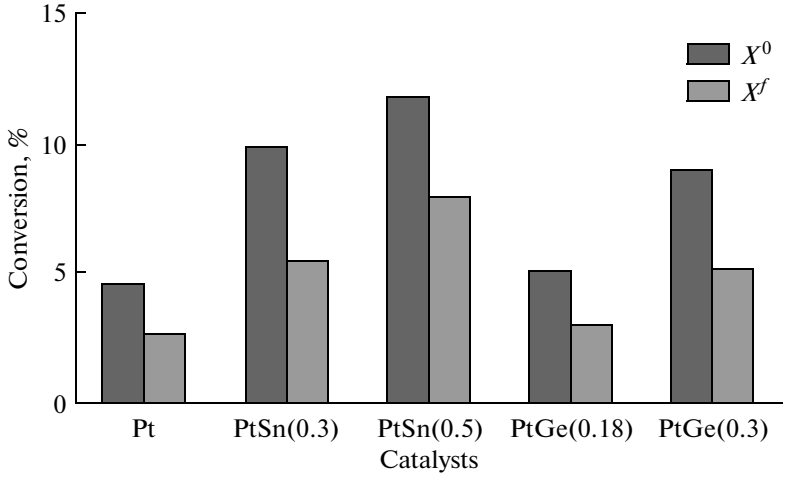

Fig. 8. Initial and final n-decane conversion for Pt/γ-A/α-A, PtSn(0.3 and 0.5 wt %)/γ-A/α-A and PtGe(0.18 and 0.3 wt %)/γ-A/α-A. X^0 – initial conversion at 10 min of the reaction time, X^f – final conversion at 120 min.

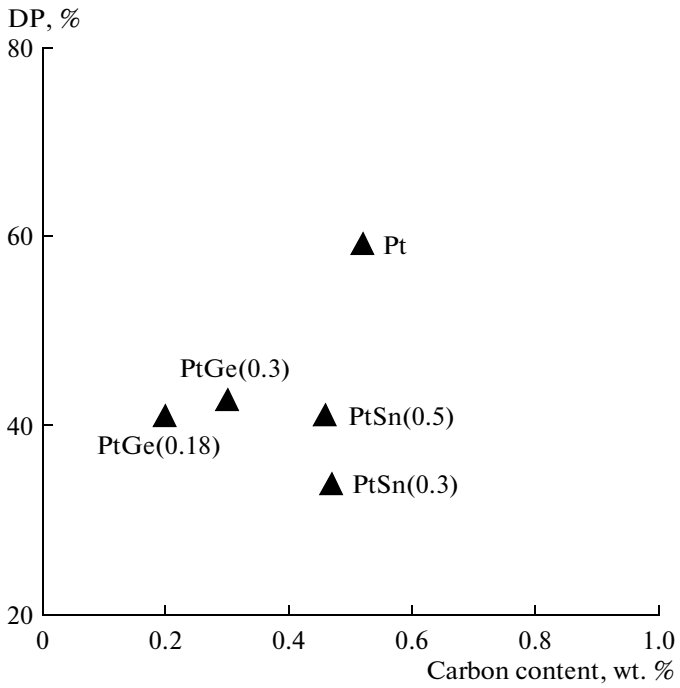

Fig. 9. Relationship between the deactivation and carbon content (measured at the end of the reaction) for Pt, PtSn and PtGe catalysts supported on γ-A/α-A.

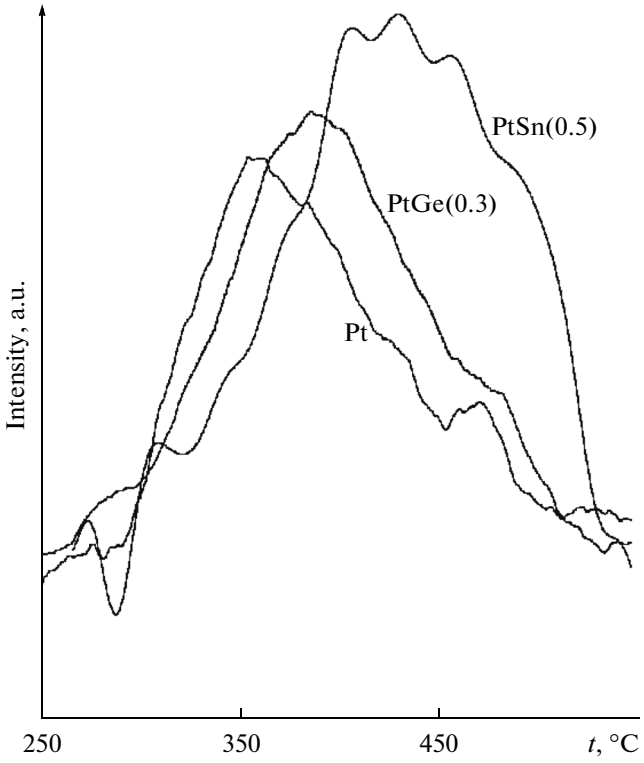

Fig. 10. TPO profiles for catalysts Pt, PtSn and PtGe supported on γ-A/α-A measured at the end of the reaction.

metallic sites [63]. Only olefins undergo cracking and isomerization reactions.

It can be observed that, the PtSn catalysts chemisorbed more hydrogen than the PtGe ones which is reflected in the higher activity (Table 1). Timofeyeva et al. [64, 65] reported that it is probable that at low H_2 chemisorption values, not all Pt centers are capable of adsorbing hydrogen but they show certain activity for the dehydrogenation of large n-paraffins, while for high hydrogen chemisorption values, the fraction of active sites capable of catalyzing this reaction increases. This would explain the difference in activity between these catalysts.

On the other hand, the apparent increase in the initial activity of the bimetallic catalysts with respect to the monometallic one may be related to the modification of the metallic phase of Pt by the second metal (Sn or Ge), either geometrically or by probable alloy formation, which results in a reduced formation of carbonaceous deposits at the beginning of the reaction. With respect to the addition of Ge, this produces an increase in the CH activation energy and a significant reduction of the R^0_{CH} in CHD reaction indicating electronic and/or geometric modifications of the metallic phase (see Table 1). This could be due to the existence of low amounts of free Pt and the alloyed phase, which would be in higher concentration when Ge is used instead of Sn. Moreover, there would also be coverage of Pt atoms by Ge or by the Pt–Ge particles or alloys, producing both the lower activity of dehydrogenation and the hydrogen chemisorption.

Figure 9 shows the deactivation parameter DP [$DP = 100\% \cdot (X^f - X^0)/X^0$, where X^0 is the initial conversion at 10 min of the reaction time and X^f is the final conversion at 120 min of the reaction time] as a function of the carbon content (wt % C) at the end of the reaction for Pt, PtSn and PtGe catalysts supported on γ-A/α-A. It can be observed that bimetallic catalysts show a lower deactivation parameter than that of the monometallic one. Besides, it can be noted that PtGe catalysts display a lower carbon deposition than PtSn ones. The latter samples show a lower deactivation than the monometallic one, despite the fact that both catalyst types display a similar carbon deposition. This behavior could be related to a different toxicity and localization of carbon in the bimetallic samples with respect to the monometallic one. Figure 10 illustrates that the TPO profile for catalyst Pt/γ-A/α-A shows a signal at lower temperature than that corresponding to the bimetallic catalysts and this could be attributed to a C deposition on the metallic phase [66–68]. PtSn and PtGe catalysts show that the TPO peak is shifted to higher temperatures, thus indicating a higher C deposition on the support [69–71]. This means that the deactivation depends not only on the coke content but also the nature and localization of the carbon.

The selectivity to 1-decene is a very important parameter, since this compound is one of the reagents

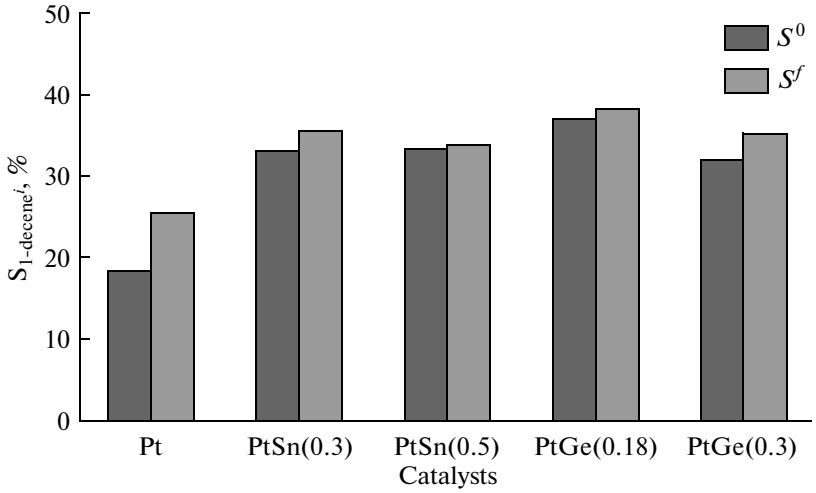

Fig. 11. Initial (S^0) and final (S^f) selectivity to 1-decene for the Pt, PtSn(0.3 and 0.5 wt %) and PtGe (0.18 and 0.3 wt %) supported on γ-A/α-A.

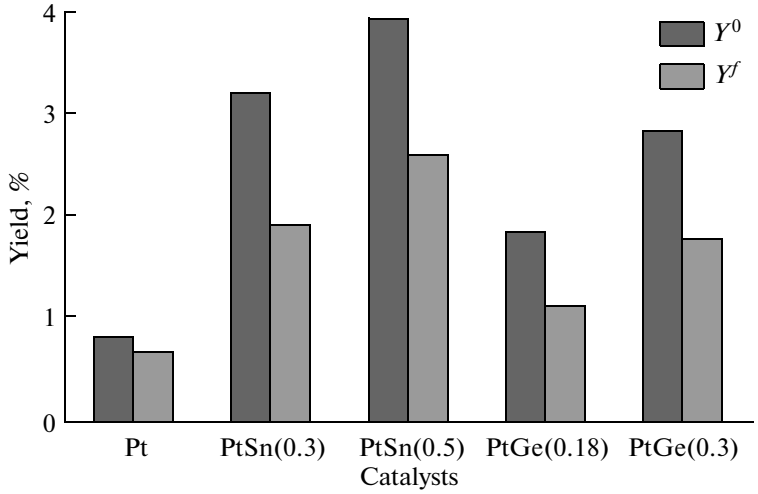

Fig. 12. Initial (Y^0) and final (Y^f) yields to 1-decene for Pt, PtSn(0.3 and 0.5 wt %) and PtGe (0.18 and 0.3 wt %) supported on γ-A/α-A.

for the production of biodegradable detergents. Fig. 11 shows the modification of the selectivity to 1-decene as a function of the reaction time for mono- and bimetallic catalysts. It can be observed that both bimetallic catalyst types are more selective to 1-decene than the monometallic one. Besides, the increase of the Sn loading has a slight effect on the selectivity. In the case of PtGe catalysts it was found that the selectivity to 1-decene was slightly higher for 0.18 wt % Ge. However, it must be noted that the selectivities of both bimetallic catalyst series were very similar. One possible explanation about the high selectivity to 1-decene of the bimetallic catalysts (PtSn and PtGe) supported on γ-A/α-A with respect to the monometallic one would be related to a decrease in the Pt-olefin interaction strength due to the presence of Sn or Ge in the vicinity of Pt, such as it was explained by other authors [9]. In this way, the successive dehydrogenation of monoolefins is decreased since they are rapidly desorbed. Consequently, the second dehydrogenation step would be limited in the bimetallic catalysts, thus being more selective to 1-decene than the monometallic one.

Figure 12 shows the initial (Y^0) and final (Y^f) yields to 1-decene defined as the product between the conversion and selectivity to 1-decene for mono- and bimetallic catalysts supported on γ-A/α-A. From these results, it can be observed that the best yield to 1-decene is obtained over PtSn(0.5 wt %) catalysts. PtGe supported catalysts show lower yields than PtSn ones, though in all cases the yields of bimetallic catalysts are higher than that of the monometallic one. It is remarkable that the catalytic performance of these catalysts is comparable to that reported in the patents [32–35].

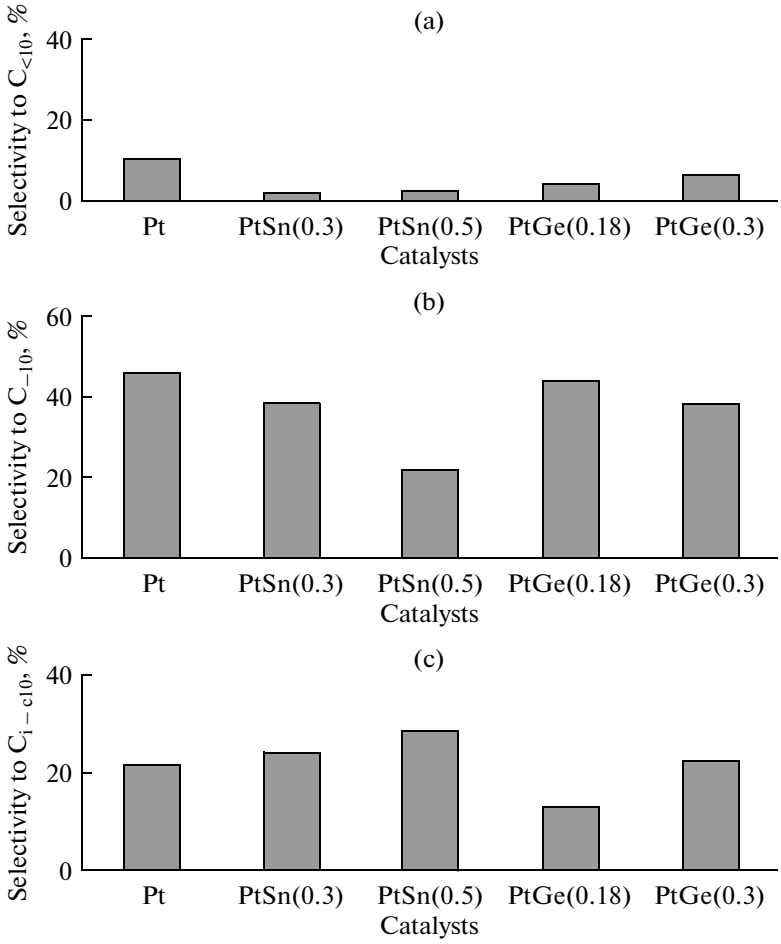

Fig. 13. Mean selectivity values to $C_{<10}$ (a), $C_{=10}$ (b) and $C_{i\text{-}c\ 10}$ (c) for Pt, PtSn(0.3 and 0.5 wt %) and PtGe (0.18 and 0.3 wt %) supported on γ-A/α-A.

Figure 13 shows the average selectivity (along the reaction time) to $C_{<10}$, $C_{=10}$ and $C_{i\text{-}c\ 10}$ for mono and bimetallic catalysts supported on γ-A/α-A. The selectivity to light paraffins ($S_{C_{<10}}$) or cracking products (Fig. 13a) for all bimetallic catalysts is lower than that for the monometallic one. The light paraffins can be produced by two different ways: acid route (cracking) or metallic route (hydrogenolysis). As mentioned above, the support (γ-A/α-A) prepared by dip coating of boehmite has a low concentration of acidic sites in comparison with γ-Al_2O_3 CK-300. This low acidic character of the support would be responsible for the low amount of cracking products. Besides, it must be indicated that Sn or Ge has a poisoning effect on the acidity of the support, mainly Sn [8, 9, 48]. It must be noted that the PtSn catalysts have a lower selectivity than PtGe ones, probably due to the different capacity of both metals to poison the acidic sites. Analizing the hydrogenolysis on the metallic sites, the Sn or Ge additions lead to catalysts with lower hydrogenolytic capacity than the monometallic one (see Table 1). Finally, the amount of Sn or Ge added to Pt has a low effect on the $S_{C_{<10}}$.

The selectivity to other monoolefins, diolefins and trienes ($S_{C_{=10}}$) is also shown in Fig. 13, b. The monometallic catalyst was more selective than the bimetallic ones, probably due to the fact that Pt improves the adsorption of monoolefins and the subsequent transformation to dienes and more unsaturated hydrocarbons. In this sense, PtSn(0.5 wt %)/γ-A/α-A shows the lowest selectivity to $C_{=10}$ of all the other bimetallic catalysts caused by the lower adsorption strength of monoolefins, but it has a high capacity to produce 1-decene. In the case of the PtGe catalyst, it can be observed that when the Ge content increases the selectivity decreases, probably because the adsorption strength is lower when the Ge concentration increases. The selectivity to non-linear hydrocarbons $C_{i\text{-}c\ 10}$ includes branched chains, isoparaffins, isooleffins, aromatics, alkyl-aromatics, etc. and it is shown in Fig. 13c. It can be observed that the Sn or Ge addition to the monometallic catalyst increases the selectivity to $C_{i\text{-}c\ 10}$, except for PtGe(0.18). As previously indicated the selectivity values are the average ones and were calculated after 10 min reaction time. During this period, the carbon deposition had an important incidence on

the catalytic properties, mainly in the monometallic catalyst. This catalyst displays a high carbon deposition in the first reaction step than the bimetallic one, thus inhibiting a higher degree of isomerization and cyclization reactions than in bimetallic catalysts for reaction times longer than 10 min. It must also be indicated that the Sn addition to Pt/Al_2O_3 catalyst has a promoting effect on the aromatization reaction, as found by Hoang Dang Lanh et al [72]. These authors observed a similar behavior using bulk Pt–Sn alloys. It is probable that the Ge addition to Pt/Al_2O_3 catalyst has a similar effect than that of the Sn addition, though in a different magnitude. According to Cortéz [73] when the Sn content increases, the conversion of olefins into aromatic compounds also increases and it does not depend on the reaction temperature in the 445–535°C range.

4. CONCLUSIONS

This work is related to a dehydrogenation process
2 of n-decane to obtain α-monoolefins using structured metallic catalysts. This technology includes an efficient method to make the washcoat on a very complex and spherical geometry. Moreover, other novelty of the support is that the thermal transformation of bohemite to gamma alumina leads to a support with a very low acidity, thus avoiding in this sense the addition of Li or other alkali metal to the support what implies an economical advantage. Finally, layered catalysts were obtained with a fewer number of elements in comparison to those mentioned in patents, what represents an economical advantage.

PtSn catalysts supported on γ-A/α-A showed better catalytic performance than the PtGe ones, this being more noticeable at higher Sn loadings. In general, PtGe bimetallic catalysts had a higher selectivity to $C_{=10}$ and produced lower amounts of non-linear chains $C_{i\text{-}c\,10}$ than the PtSn ones.

ACKNOWLEDJMENTS

The authors wish to acknowledge the financial support received from Universidad Nacional del Litoral and ANPCYT-Argentina. They also thank Miguel Torres for his experimental assistance.

REFERENCES

1. Pujadó, P.R., UOP Pacol dehydrogenation process, in *Handbook of Petroleum Refining Processes: Copyrighted Material,* The McGraw-Hill Companies, Inc., 1986, 1997, 2004.
2. Kocal, J.A., Vora, B.V., and Imai, T., *Appl. Catal. A: General,* 2001, vol. 221, pp. 295–301.
3. Gattuso, M.N., Vora, B.V., and Imai, I., *Chem. Age of India,* 1996, vol. 6, p. 37.
4. Growth in household detergents is driving demand for linear alkylbenzene produced from kerosene-derived normal paraffins – http://www.uop.com/processing-solutions/petrochemicals/detergents/#lab.
5. Podkletnova, N.M., Kogan, S.B., and Bursian, N.R., *Zh. Priklad. Khim.,* 1987, vol. 60, no. 9, p. 2028.
6. Castro, A.A., *Catal. Lett.,* 1993, vol. 22, p. 123.
7. Gokak, D.T., Basrur, A.G., Rajeswar, D., Rao, G.S., and Krishnamurthy, K.R., *React. Kinet. Catal. Lett.,* 1996, vol. 59, no. 2, p. 315–323.
8. Sterligov, O.D., Solov'yev, V.M., and Isagulyants, G.V., *Petroleum Chem. U.R.S.S.,* 1980, vol. 20, no. 3, pp. 134–140.
9. García Cortez, G., de Miguel, S.R., Scelza, O.A., and Castro, A.A., *Actas de XIII Simposio Iberoamericano de Catálisis, Segovia,* 1992, vol 1, pp. 379–382.
10. Padmavathi, G., Chaudhuri, K.K., Rajeshwer, D., Rao, G.S., Krishnamurthy, K.R., Trivedi, P.C., Hathi, K.K., Subramanyam, N., *Chem. Eng. Sci.,* 2005, vol. 60, pp. 4119–4129.
11. Sanfilippo, D. and Miracca, I., *Catal. Today,* 2006, vol. 111, pp. 133–139.
12. Xioading, X. and Moulijn, J.A., *Structures Catalysts and Reactors,* CRC Taylor & Francis, 2005, p. 751.
13. Groppi, G., Ibashi, W., Tronconi, E., and Forzatti, P., *Chem. Ing. J.,* 2001, vol. 82, pp. 57–71.
14. van der Puil, N., Dautzenberg, F.M., van Bekkum, H., and Jansen, J.C., *Microp. and Mesop. Mat.,* 1999, vol. 27, pp. 95–106.
15. Agrafiotis, C. and Tsetsekou, A., *J. of the Euro. Ceram. Soc.,* 2000, vol. 20, pp. 815–824.
16. Agrafiotis, C. and Tsetsekou, A., *J. of the Euro. Ceram. Soc.,* 2000, vol. 20, pp. 825–834.
17. Meille, V., Pallier, S., Santa Cruz Bustamante, G.V., Roumanie, M., and Reymond, J.-P., *Appl. Catal. A: General.,* 2005, vol. 286, pp. 232–238.
18. Meille, V., *Appl. Catal. A: General.,* 2006, vol. 315, pp. 1–17.
19. Burton, J.J. and Garten, R.L., *Advanced Materials in Catalysis,* London: Academic Press, 1977, pp. 307.
20. Wu, X., Weng, D., Xu, L., and Li, H., *Surf. and Coat. Technol.,* 2001, vol. 145, pp. 226–232.
21. Zhao, S., Zhang, J., Weng, D., and Wu, X., *Surf. and Coat. Tech.,* 2003, vol. 167, pp. 97–105.
22. Shigapov, A.N., Graham, G.W., McCabe, R.W., Peck, M.P., and Plummer, H.K., *Appl. Cat. A: General.,* 1999, vol. 182, pp. 137–146.
23. Ballarini, A.D., Zgolicz, P., Vilella, I.M.J., de Miguel, S.R., Castro, A.A., and Scelza, O.A., *Appl. Cat. A: General.,* 2010, vol. 381, pp. 83–91.
24. Cristiani, C., Valentini, M., Merazzi, M., Neglia, S., and Forzatti, P., *Catal. Today,* 2005, vol. 105, pp. 492–498.
25. Montanaro, L. and Saracco, G., *Ceram. Internat.,* 1995, vol. 21, pp. 43–49.
26. Vural, M., Zeytin, S., and Ucisik, A.H., *Surf. and Coat. Tech.,* 1997, vol. 97, pp. 347–354.
27. Perego, C. and Villa, P., *Catal. Today,* 1997, vol. 34, pp. 281–305.
28. Valentini, M., Groppi, G., Cristiani, C., Levi, M., Tronconi, E., and Forzatti, P., *Catal. Today,* 2001, vol. 69, pp. 307–314.

29. Valentini, M., Nichio, N., Groppi, G., Cristiani, C., Tronconi, E., and Forzatti, P., *Actas del XIII JAC 2003 y 2do MercoCat,* Argentina, 2003.
30. S. Kawagoshi and K. Funabiki, Pat. 3947340 USA, Method for forming γ-alumina coating on refractory article, Publ. March 30, 1976.
31. Valdez-Sols, T., Marban, G., and Fuertes, A.B., *Microp. Mesop. Mater.,* 2001, vol. 43, pp. 113–126.
32. Jensen, R.H., Bricker, J.C., Chen, Q., et al., Pat. 6177381 USA, Layered catalyst composition and processes for preparing and using the composition, UOP LLC, Des Plaines, IL (USA), Publ. Jan. 23, 2001.
33. Rende, D.E., Broerman, A.W., Bozzano, A.G., and Lawson, R.J., Pat. 6756515 USA, Dehydrogenation process using layered catalyst composition, UOP LLC, Des Plaines, IL (USA), Filed Oct. 25, 2002, Publ. Jun. 29, 2004.
34. Dongara, R., Basrur, A.G., Gokak, D.T., Rao, K.V., Krishnamurthy, K.R., and Bhardwaj, I.S., Pat. 5677260 USA, Catalyst composite for dehydrogenation of paraffins to mono-olefins and method for the preparation thereof, Indian Petrochemicals Corporation Limited. Publ. Oct. 14, 1997.
35. Uzio, D., Didillon, B., and Pellier, E., Pat. 6498280 USA, Catalyst comprising an element from groups 8, 9 or 10 with good accessibility, and its use in a paraffin dehydrogenation process, Institut Francais du Petrole (FR), Filed Apr. 25, 2000, Publ. Dec. 24, 2002.
36. Park, Y.K., Tadd, E.H., Zubris, M., and Tannenbaum, R., *Materials Research Bulletin,* 2005, vol. 40, pp. 1506–1512.
37. Yasaki, S., Yoshino, Y., Ihara, K., and Ohkubo, K., Pat. 5208206, USA, May 4, 1993.
38. Cinneide, A.D. and Clarke, J.K.A., *Catal. Rev.,* 1972, vol. 7, p. 233.
39. Balandin, A.A., *Zh. Fiz. Khim.,* 1957, vol. 31, p. 745.
40. van Schaik, J.R.H., Dessing, R.P., and Ponec, V., *J. Catal.,* 1975, vol. 38, pp. 273–282.
41. Boudart, M., *Adv. Catal.,* 1969, vol. 20, pp. 153–166.
42. Gault, F.G., *Adv. Catal.,* 1981, vol. 30. pp. 1–95.
43. Biloen, B., Helle, J.N., Verbeek, H., Dautzembverg, F.M., Sachtler, W.M.H., *J. Catal.,* 1980, vol. 63, p. 112.
44. Wagner, C.D., Riggs, W.M., Davis, L.E., Moulder, J.F., and Muilenberg, G.E., *Handbook of X-ray Photoelectron Spectroscopy,* Perkin-Elmer Corp., Phys. Electr. Division, 1979.
45. McNicol, B.D., *J. Catal.,* 1977, vol. 46, pp. 438–440.
46. Wagstaff, N. and Prins, R., *J. Catal.,* 1979, vol. 59, pp. 434–445.
47. Mariscal, R., Fierro, J.L.G., Yori, J.C., Parera, J.M., and Grau, J.M., *Appl. Catal. A: General.,* 2007, vol. 327, pp. 123–131.
48. Goldwasser, J., Arenas, B., Bolivar, C., Rodríguez, A., Fleitas, A., Giron, J., and Castro, G., *J. Catal.,* 1986, vol. 100, pp. 75–85.
49. Bouwman, R. and Biloen, P., *J. Catal.,* 1977, vol. 48, pp. 209–216.
50. De Miguel, S.R, Scelza, O.A., and Castro, A.A., *Appl. Catal.,* 1988, vol. 44, pp. 23–32.
51. Borgna, A., Garetto, T.F., Apesteguia, C.R., and Moraweck, B., *Appl. Catal. A: General.,* 1999, vol. 182, pp. 189–197.
52. Llorca, J., Ramirez de la Piscina, P., Fierro, J.-L.G., Sales, J., and Homs, N., *J. Mol. Catal. A: Chemical.,* 1997, vol. 118, pp. 101–111.
53. Hatch, L.F. and Matar, S., *From Hydrocarbons to Petrochemicals,* Houston: Gulf Publishing Company, 1981.
54. De Miguel, S.R., Castro, A.A., Scelza, O.A., Fierro, J.L.G., and Soria, J., *Catal. Lett.,* 1996, vol. 36, pp. 201–206.
55. De Miguel, S.R., Bocanegra, S.A., Vilella, I.M.J., Guerrero-Ruiz, A., and Scelza, O.A., *Catal. Lett.,* 2007, vol. 119, pp. 5–15.
56. Vatcha, S.R., Trifiro, F., and Cavani, F., *Oxidative Dehydrogenation and Alternative Dehydrogenation Processes,* Helios, D., Ed., Catalytica Studies Division, 1993, no. 4992 OD.
57. *Dehydrogenation Processes,* Helios, D., Ed., Catalytic Study no. 4992, OD, USA, 1993.
58. Bosch, P., Valenzuela, M.A., Zapata, B., Acosta, D., Aguilar-Ríos, G., Maldonado, C., and Shifter, I.J., *J. Molec. Catal.,* 1994, vol. 93, pp. 67–78.
59. Bocanegra, S.A., Guerrero-Ruíz, A., de Miguel, S.R., and Scelza, O.A., *Appl. Catal. A: General.,* 2004, vol. 277, pp. 11–22.
60. Ballarini, A.D., Ricci, C.G., de Miguel, S.R., and Scelza, O.A., *Catal. Today,* 2008, vol. 133, pp. 28–34.
61. Bocanegra, S.A., Ballarini, A.D., Scelza, O.A., and de Miguel, S.R., *Mat. Chem. and Phys.,* 2008, vol. 111, pp. 534–541.
62. Bocanegra, S., Ballarini, A., Zgolicz, P., Scelza, O., and de Miguel, S., *Catal. Today,* 2009, vol. 143, pp. 334–340.
63. Tyupaev, A.P., Timofeeva, E.A., and Isagulyantz, G.V., *Nefteknimiya,* 1981, vol. 21, no. 2, pp. 186–190.
64. Timofeyeva, E.A., Tyupaev, A.P., and Isagulyants, G.V., *Izv. Akad. Naúk SSSR. Ser. Khim.,* 1981, vol. 9, p. 2067.
65. Timofeyeva, Ye.A., Bryukhanov, V.G., and Isagulyants, G.V., *Petrol. Chem. U.S.S.R.,* 1981, vol. 21, pp. 77–81.
66. Caruso, F., Jablonski, E.L., Grau, J.M., and Parera, J.M., *Appl. Catal.,* 1989, vol. 51, pp. 195–202.
67. Zharkov, B.B., Galperin, L.B., Medzkinskii, V.L., Butochnikova, L.F., Krasilnikov, A.N., and Yakovleva, I.D., *React. Kinet. Catal. Lett.,* 1986, vol. 32, pp. 457–462.
68. Barbier, J., Churin, E.J., Parera, J.M., and Riviere, J., *React. Kinet. Catal. Lett.,* 1985, vol. 29, p. 323.
69. Siri, G.J., Bertolini, G.R., Casella, M.L., and Ferretti, O.A., *Mat. Lett.,* 2005, vol. 59, pp. 2319–2324.
70. Siri G.J., Casella, M.L., Ferretti, O.A., and Fierro, J.L.G., *Stud. in Surf. Sc. and Cat.,* 2001, vol. 139, pp. 287–294.
71. Casella, M.L., Siri, G.J., Santori, G.F., and Ferretti, O.A., *Langmuir,* 2000, vol. 16, pp. 5639–5643.
72. Lanh, H.D., Lietz, G., Thoang, Ho, Si, and Völter, J., *React. Kinet Catal. Lett.,* 1982, vol. 21, p. 429.
73. García Cortéz, G., *Doctoral Thesis,* Argentina: INCAPE-FIQ-UNL, 1992.

SPELL: 1. Analizing, 2. monoolefins